

RESEARCH ARTICLE | JUNE 03 2021

Aqueous choline amino acid deep eutectic solvents

Special Collection: [Chemical Physics of Deep Eutectic Solvents](#)

Shurui Miao ; Haihui Joy Jiang ; Silvia Imberti ; Rob Atkin ; Gregory Warr  



J. Chem. Phys. 154, 214504 (2021)

<https://doi.org/10.1063/5.0052479>



View
Online



Export
Citation

CrossMark



The Journal of Chemical Physics

Special Topic: Algorithms and Software for Open Quantum System Dynamics

Submit Today

Aqueous choline amino acid deep eutectic solvents

Cite as: *J. Chem. Phys.* **154**, 214504 (2021); doi: 10.1063/5.0052479

Submitted: 31 March 2021 • Accepted: 14 May 2021 •

Published Online: 3 June 2021



View Online



Export Citation



CrossMark

Shurui Miao,¹ Haihui Joy Jiang,¹ Silvia Imberti,² Rob Atkin,³ and Gregory Warr^{1,a)}

AFFILIATIONS

¹School of Chemistry and Sydney Nano Institute, The University of Sydney, NSW 2006, Australia

²STFC, ISIS Neutron and Muon Source, Rutherford Appleton Laboratory, Didcot OX11 0QX, United Kingdom

³School of Molecular Sciences, The University of Western Australia, WA 6009, Australia

Note: This paper is part of the JCP Special Topic on Chemical Physics of Deep Eutectic Solvents.

a) Author to whom correspondence should be addressed: gregory.warr@sydney.edu.au

ABSTRACT

We have investigated the structure and phase behavior of biocompatible, aqueous deep eutectic solvents by combining choline acetate, hydrogen aspartate, and aspartate amino acid salts with water as the sole molecular hydrogen bond donor. Using contrast-variation neutron diffraction, interpreted via computational modeling, we show how the interplay between anion structure and water content affects the hydrogen bond network structure in the liquid, which, in turn, influences the eutectic composition and temperature. These mixtures expand the current range choline amino acid ionic liquids under investigation for biomass processing applications to include higher melting point salts and also explain how the ionic liquids retain their desirable properties in aqueous solution.

Published under an exclusive license by AIP Publishing. <https://doi.org/10.1063/5.0052479>

INTRODUCTION

Since they were first reported by Abbott *et al.*,¹ deep eutectic solvents (DESs) have emerged as an important class of green solvents with the potential to replace many widely used volatile organic compounds in research and industry. DESs are mixtures with abnormally low eutectic temperatures, not only significantly lower than melting points of their constituents but also below the predicted melting point depression due to ideal mixing.^{2–5} This behavior is exemplified by reline, a 1:2 mol:mol (anhydrous) mixture of choline chloride ($T_m = 323^\circ\text{C}$) and urea ($T_m = 133^\circ\text{C}$),⁶ which melts just above room temperature ($T_m = 25^\circ\text{C}$).⁷ Structural studies have confirmed the formation of a complex and extensive hydrogen bonding network involving the choline cation, chloride anion, and urea hydrogen-bond donor (HBD) in which the delicate balance of forces between all species suppresses crystallization.^{8–10}

Despite the vast number of combinations hypothesized, the majority of the very many studies of DESs carried out over the past two decades have involved choline chloride (ChCl).¹¹ It has become the most well-known quaternary ammonium salt for DES formulation. While many studies seek to establish a comprehensive understanding of structure–property relationships and design rules for ChCl-based DESs,^{8,10,12,13} here, we ask how changing anion can affect the DES formation and structure, and whether our

understanding of ChCl-based DESs can be generalized to systems containing other choline salts.

Choline carboxylate and amino acid salts immediately stand out as promising candidates. Since their discovery, these salts have been recognized by the ionic liquid (IL) community as renewable and non-toxic, biocompatible ILs.^{14–16} A number of studies have been performed to characterize their structure and the molecular origin of their physicochemical properties.^{17,18} Although many of these choline salts are room temperature liquids, some of them such as choline aspartate have melting points above 90°C .¹⁹ In our recent small-angle x-ray scattering study, we showed that changing the anion can affect not only the liquid nanostructure of these ILs but also their miscibility with various molecular liquids and the structure of those mixtures.²⁰

Many choline salts also have very high viscosities in the pure molten state,¹⁹ posing challenges for them to be handled as pure liquids and compromising their uptake for large-scale applications. Together with the cost consideration, it is not surprising that such applications, including for treatment of biomass and coal, employ choline salt–water mixtures.^{21–24} This is often at such a low water content (<50 wt. %) that the mixture cannot be regarded simply as an aqueous electrolyte solution. While water is commonly treated as a green and cheap diluent, it is also a paragon among hydrogen bonding species. In their study of water dilution of reline, Hammond

et al. showed that its key DES features are preserved at up to 1:10 mol reline:water. At a low water content (1:1 mol ratio), water was even shown to modestly reinforce the choline–urea H-bonding, possibly enhancing the melting point depression in DESs.^{25,26}

Here, we examine a set of simplified, two-component mixtures, consisting of choline acetate, hydrogen aspartate, or aspartate in combination with water as the sole HBD. In choline-based ionic liquids, the anion structure strongly affects the liquid nanostructure and functionality.^{20,27} We thus seek to understand how polyatomic, organic anions in combination with water can be used to control the structure and properties of biocompatible choline salts in both ILs and DESs.^{28,29}

MATERIALS AND METHODS

Choline acetate (ChAc), choline aspartate (Ch₂Asp), and choline hydrogen aspartate (ChHAsp) were prepared by neutralization of choline hydroxide with the corresponding acid. DL-aspartic acid (>99%, Fluka), acetic acid (HPLC, VWR), and choline hydroxide aqueous solution (~46 wt.%, Aldrich) were used as received. The concentration of choline hydroxide solution was determined through titration before use. The base was diluted to 20 wt. % and mixed dropwise with a 20 wt. % solution containing the corresponding acid. The reaction was kept on an ice bath (<10 °C) and stirred overnight under ambient conditions. Upon completion, a clear aqueous solution is obtained. Bulk water was removed on a rotary evaporator (40 °C, 10 mbar), and drying of the residual water was performed under high vacuum (200 μbar) at room temperature for >48 h. The water content of the final product was confirmed by weight to be <1 wt. %. The dried salts have a light amber appearance due to a trace amount of impurity from the choline hydroxide reagent (undetectable by ¹H NMR).

d₉-salts were prepared from d₉-choline chloride (d₉-ChCl, 98%, Cambridge Isotope) by ion-exchange (Amberlite IRA-400 for hydroxide, 25 ml) to d₉-choline hydroxide (d₉-ChOH). Before use, resins were washed with concentrated NaOH aqueous solutions five times. A silver test (0.2M AgNO₃ and 0.25M HNO₃ in water) confirmed that a negligible amount of chloride remained in the resins after which water (Milli-Q) rinses were performed until pH returned to neutral. 5 g of d₉-ChCl was dissolved in 50 ml of H₂O/methanol 1:1 v/v mixture and loaded onto 200 ml of resins using the same solvent mixture as the eluent. The eluent was collected in fractions, and all those with basic pH (>7.5) were combined. A small volume of the obtained solution was titrated to determine the concentration

of ChOH. d₉-salts were prepared identically to hydrogenous choline salts with hydrogenous acids.

d₁₂- and d₃-salts were obtained by H/D exchange of exchangeable protons within d₉-salts and hydrogenous salts. Deuterium oxide D₂O (99%, Cambridge Isotope) was added to a pre-exchange salt in a 3:1 volume ratio. The resulting mixture was stirred for 5 min before drying on a rotary evaporator (40 °C, 10 mbar). Mass was monitored to ensure that bulk D₂O was removed. This process was repeated five times, and the final sample was dried under high vacuum (200 μbar) at room temperature for >48 h. All samples were sealed and stored under nitrogen.

Molecular structures and compositions of mixtures of choline acetate (ChAc), choline aspartate (Ch₂Asp), and choline hydrogen aspartate (ChHAsp) with water are shown in Fig. 1. Samples for neutron diffraction were prepared by mass to yield identical molar compositions with all isotopic substitution patterns. Neutron diffraction patterns were collected on the SANDALS beamline at the ISIS Neutron and Muon Source (Rutherford Appleton Laboratories, UK). Neutron wavelengths used range between 0.05 and 4.95 Å, allowing access to the q-range between 0.05 and 50 Å⁻¹. Samples were contained in null scattering Ti_{0.68}Zr_{0.32} flat plate cells with a total capacity of 1 ml. All samples were measured under vacuum at 296 K for 6 h each. Mass was monitored to ensure no loss of sample under vacuum. Data reduction was performed using GUDRUN according to local procedures using experimental densities of all samples at 25 °C.³⁰ The empirical potential structure refinement (EPSR) package was used to fit the normalized experimental diffraction data.³¹ Atom labeling and initial Lennard-Jones parameters are provided in the [supplementary material](#) (Fig. S1 and Table S1). Each simulation box was refined to fit all four diffraction patterns on chemically identical samples with different isotopic substitutions simultaneously, as shown in Fig. 2, and the size of the simulation box was always more than twice the size of the largest experimental structural feature (>60 Å; box compositions and dimensions shown in Table S3). All analyses were performed over >1000 frames of data accumulation after convergence.

Differential scanning calorimetry was performed on a DSC823^o (Mettler Toledo) instrument with a liquid nitrogen adaptor. Samples of the desired water content were prepared by mass and cycled between -140 and 100 °C at 15 K/min to obtain the sub-zero melting point. The presence of clear liquid phases beyond the measured liquidus temperature is confirmed by visual observation at -20 and -80 °C, and samples were stored in -20 and -80 °C freezers for

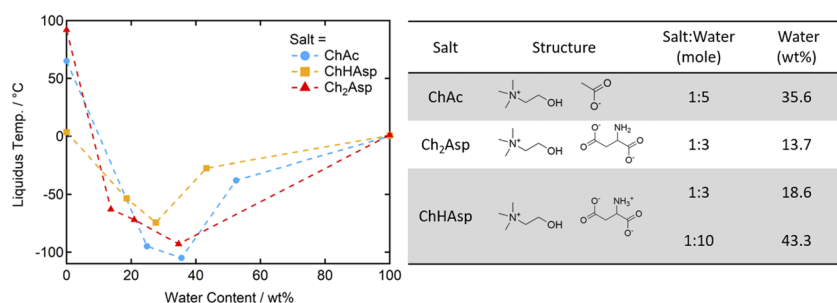


FIG. 1. Liquidus temperature of various choline salt + water mixtures measured using differential scanning calorimetry. The mixtures have mole ratios of salt:water = 1:3, 1:5, and 1:10. Dashed lines between markers are added to guide the eye. The table shows the compositions of the four systems studied in detail by neutron diffraction.

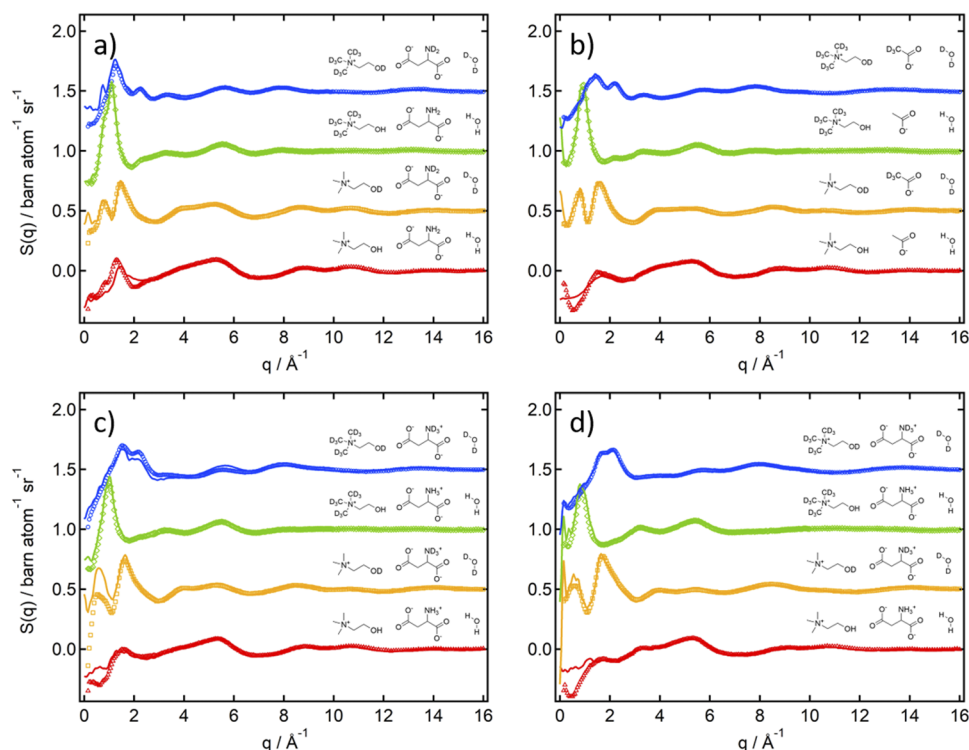


FIG. 2. Experimental (hollow circles) and fitted (solid lines) neutron diffraction patterns between 0 and 16 \AA^{-1} of mixtures of choline salt–water at various mole ratios and with four different H/D isotopic labeling patterns, shown above each curve. The four systems are denoted as follows: (a) choline aspartate + $3 \text{ H}_2\text{O}$, (b) choline acetate + $5 \text{ H}_2\text{O}$, (c) choline hydrogen aspartate + $3 \text{ H}_2\text{O}$, and (d) choline hydrogen acetate + $10 \text{ H}_2\text{O}$. Diffraction patterns have been offset for clarity, and the corresponding deuteration patterns are shown.

>48 h before the visual confirmation was made. The liquidus temperature of each mixture is obtained as the maxima in the melting endotherms.

RESULTS AND DISCUSSION

Figure 1 shows the melting points (liquidus lines) of mixtures of choline acetate (ChAc), choline aspartate (Ch₂Asp), and choline hydrogen aspartate (ChHAsp) with water at mol/mol ratios of 1:3, 1:5, and 1:10. The result clearly reveals a massive depression in melting points, up to 100°C lower than pure water, significantly larger than the predicted value by available thermodynamic models.¹¹

Although quite similar in their mass compositions, the eutectics of the three mixtures represent very different salt:water mole ratios, as shown in Fig. 1. In order to understand the details of the liquid structure in these mixtures, we have compared neutron diffraction patterns of the model system choline acetate + 5 water (35.6 wt. % water) with three different choline aspartate + water mixtures at various mole ratios (see the table of Fig. 1). As aspartic acid contains two carboxylate groups, it can exist in both di-anion, $[\text{Asp}^{2-}]$, and monoanion, $[\text{HAsp}^-]$, forms. The latter is a zwitterion with both carboxylate groups deprotonated and the α -amino group protonated (see Fig. 1 and Table S2),^{18,32} which we have examined at two water mole ratios: 1:3 and 1:10 mol/mol.

Figure 2 shows the experimental neutron diffraction patterns of four choline salt–water mixtures. Each consists of four distinct H/D isotopic substitution patterns and shows best fits obtained from a single converged liquid model using the empirical potential structure refinement package.³¹ The fitted diffraction patterns are in good agreement with the experiment, except near the resolution limit ($\sim 0.2 \text{ \AA}^{-1}$) where some errors in the correction of inelastic scattering leads to discrepancies. This is most evident for choline aspartate + 3 water as the pure salt is extremely hygroscopic. A small amount of adventitious hydrogenous water from air (during sample storage and handling) is also the likely cause of the observed low intensity of the low- q peak in the $d_1\text{Chd}_3\text{Asp} + \text{D}_2\text{O}$ mixture [Fig. 2(c)]. However, as EPSR provides atomic resolution, the structural refinement is performed on the molecular scale, and best fit is obtained across four distinct contrasts, our interpretation should not be affected.

The most striking experimental structural feature is a sharp peak near 1 \AA^{-1} , which occurs in all systems in which *only* choline trimethylammonium is deuterated ($d_9\text{-Ch}$). This corresponds to a real space separation of $\sim 6 \text{ \AA}$, comparable to the size of anions, which arises from the average nearest neighbor separation between choline cations. These diffraction patterns also clearly show that lower angle peaks corresponding to long-range periodicities ($q < 0.5 \text{ \AA}^{-1}$, indicative of the amphiphilic liquid nanostructure as is commonly seen

in a variety of ionic liquids and some DESs) are absent from all systems.^{17,33}

We first examine molecular arrangements and intermolecular interactions in the simpler choline acetate system to elucidate choline–carboxylate, choline–water, and carboxylate–water interactions and then explore how the more complex amino acid aspartate and its speciation state affect the nanostructure and hydrogen bonding in these liquid mixtures.

Choline acetate + 5 water

Figure 3 shows partial pair correlation and spatial distribution functions between key component atoms in this mixture. Correlations between the cationic, quaternized ammonium charged center of choline and carboxylate or water oxygens both yield broad nearest neighbor peaks of similar heights near 5 Å separation. Both also yield very similar spatial distribution functions, confirming that the quaternary ammonium of choline does not effectively differentiate between ion–ion and ion–dipole interactions with carboxylate and water, respectively.

In contrast, the formation of H-bonds is highly selective. Hydrogens on both the choline hydroxyl group and water form strong H-bonds with carboxylate oxygens, shown by the pronounced nearest neighbor correlation peaks at a characteristic

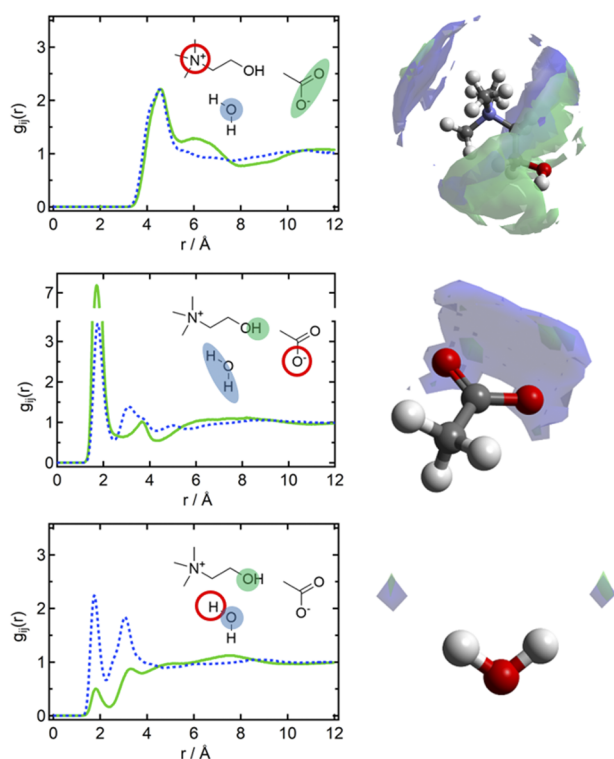


FIG. 3. Pair correlation functions of electrostatic and H-bonding interactions between a central atom (circled) and other functional group atoms in the choline acetate + 5 water system, together with spatial distribution functions. The probability surfaces enclose the most likely (top 15%) locations for the surrounding species around the central atom (color coded).

distance of 1.8 Å. The choline hydroxyl oxygen, however, is a much weaker H-bond acceptor than water, indicating that H-bonds to it are rare. This result also confirms that the choline hydroxyl–carboxylate H-bond is strong enough to persist among water networks, consistent with past studies of choline-based ILs and their water mixtures.^{22,34,35}

The water–water pair correlation function also exhibits a pronounced second peak at 3 Å, arising from an ordered arrangement of next-nearest neighbor water molecules. Together with a pronounced primary correlation at the preferred H-bond distance of 1.8 Å, this is evidence that a tetrahedral H-bond network similar to bulk water is present in 1:5 ChAc:water.^{35–37} These results enable us to rank H-bond acceptor oxygens as follows: carboxylate > water > hydroxyl. That is, any HBD will prefer to H-bond first with carboxylate, followed by water. This implies that addition of water in this system beyond the capacity of carboxylates will enhance the water network, leading it to act as a diluent.

A similar phenomenon has been seen in DESs containing choline chloride. As reported by Hammond *et al.*, the unusually low melting point of reline is a consequence of an extensive H-bond network between urea and choline chloride.⁸ The interactions are optimized when the chloride anion is surrounded on average by two urea molecules and one choline cation. The delicate balance of strong intermolecular interactions involving all species is sufficient to suppress crystallization, yielding a liquid at much lower temperatures than ideal mixing alone. H-bonds around the chloride anion are shown to have the highest priority, resulting in choline and the HBD working synergistically to wrap around a chloride anion by both H-bonding and electrostatic interactions.^{8,12} Small amounts of added water can enhance the existing H-bond network around chloride by providing an excess of H-bond acceptors. However, further addition of water will trigger a competition between the water–DES H-bond and the weakest DES–DES H-bond (often between HBDs), disrupting an essential feature of the DES and leading to its effective dissolution in water.^{12,25,38}

If the formation of an H-bond network is critical to the formation of a DES, as suggested from investigations of H-bonding structures in reline and other DESs, then the eutectic composition of choline carboxylate–water systems should depend on carboxylate acceptor availability on the anion.

Choline acetate contains a single H-bond donor on the cation hydroxyl but six potential acceptor sites, assuming two on each of the cation and anion oxygens. Figure 3 confirms that all these H-bonds occur in choline acetate + 5 water, but the surfeit of acceptor sites prevents ChAc alone from forming an extended H-bond network. As water has two donor and two acceptor sites, we can estimate the minimum number of water molecules (or any HBD) necessary to saturate the available H-bonding sites, enabling the salt to be integrated into an extended H-bond network. If all five H-bond acceptor sites are occupied by a water H-bond donor without concern for steric constraints, this leads to an expected minimum mole ratio of ChAc:H₂O = 1:2.5. Full hydration of course yields 1:5. This is consistent with the experimental eutectic composition (Fig. 1), which lies between 1:3 and 1:5, and the observed features of the liquid structure (Fig. 3) at ChAc:H₂O = 1:5. The presence of water–water H-bonds and tetrahedral water at this composition reflects the full hydration condition and also that the H-bond network includes many different local structures.

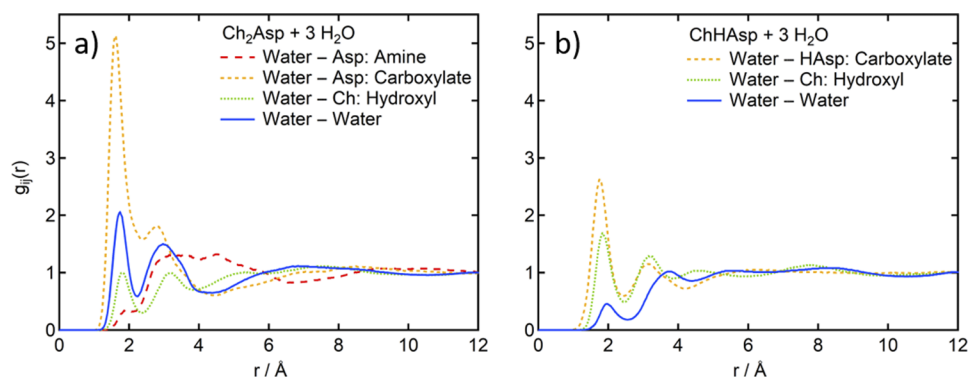


FIG. 4. Atom-atom pair correlation functions between the hydrogen on water and all H-bond acceptors in (a) choline hydrogen aspartate + 3 water and (b) choline aspartate + 3 water. In ChHAsp, the ammonium nitrogen is protonated and cannot act as an H-bond acceptor.

Choline aspartate salts

Many of the key electrostatic and H-bonding interactions seen in choline acetate + water are largely preserved in both choline hydrogen aspartate (ChHAsp) and choline aspartate (Ch₂Asp) systems (see Figs. 4 and 6 and Fig. S2). Carboxylate groups are both deprotonated in both anion species. The α -amino group provides the main structural difference through additional two H-bond donors and one acceptor on Asp²⁻ or three donors on HAsp⁻. This can lead to anion-anion H-bonding in pure choline amino acid ionic liquids.^{17,34,39} The amine nitrogen is an ineffective H-bond

acceptor, especially in the presence of water (Fig. S3). However, as we will show below, H-bonds in which the α -amine is the donor, and particularly those where the cationic ammonium group is present (i.e., ChHAsp), play a critical role in determining molecular arrangements within the liquid.

Following the same approach used for choline acetate yields an excess of eight H-bond acceptor sites on Ch₂Asp (including the α -amine donors only) and six on ChHAsp. The corresponding water ratios for minimal and complete solvation are thus $4 < \text{Ch}_2\text{Asp}:\text{H}_2\text{O} < 8$ and $3 < \text{ChHAsp}:\text{H}_2\text{O} < 6$. While not predictive, these estimates are consistent with the experimental eutectic compositions shown

TABLE I. Average coordination number of all H-bonds in Ch₂Asp and ChHAsp systems (pair correlation functions shown in Fig. 6) calculated using a separation cutoff of 2.5 Å with respect to one hydrogen on the H-bond donor.

H-bond		Ch ₂ Asp		ChHAsp	
Donor hydrogen	Acceptor	1:3	1:3	1:10	1:10
		0.10	0.12	0.07	
		0.62	0.59	0.38	
		0.28	0.11	0.43	
		0.02	0.02	0.00	
		0.91	1.02	0.52	
		0.13	0.14	0.58	
		0.12	0.07	0.03	
		0.26	0.79	0.41	
		0.24	0.23	0.78	

in Fig. 1 and support the idea that the eutectic is related to the HBD's capacity to enable an extended H-bond network throughout the liquid. We first compare the liquid structure in two “water lean” samples with 1:3 salt:HBD mole ratios, choline hydrogen aspartate + 3 water and choline aspartate + 3 water and then a “water rich” composition, choline hydrogen aspartate + 10 water.

The atom–atom pair correlation functions in Fig. 4 show that the water hydrogen is strongly H-bonded to carboxylate oxygens in both water lean systems, with clear peaks at an H-bond length of 1.8 Å. This agrees with the results reported above for the choline acetate system and with other previous studies.^{17,34} As noted above, the deprotonated α -amino group of Ch₂Asp is available as an H-bond acceptor site but is an uncommon interaction with normalized

atom-pair correlation peak well below 1 at 1.8 Å. It thus has a negligible impact on water–ion H-bonds. The rarity of this H-bond not due to the lack of H-bond donors but due to the α -amino group is a weak H-bond acceptor, as has been consistently identified previously.^{17,22,34,35} Addition of more water will likely expand the water network rather than forming more water–ion H-bonds, as observed for the hydroxyl oxygen of choline in ChAc + 5 water above.

Next-nearest neighbor peaks are also present in pair correlation functions of H-bonds to carboxylate oxygens. Unlike the water network, this is imposed by the sp^2 geometry of the functional group dictating the location of the second oxygen.

There is a marked difference in water–water correlations between these two water lean systems. The miniscule nearest

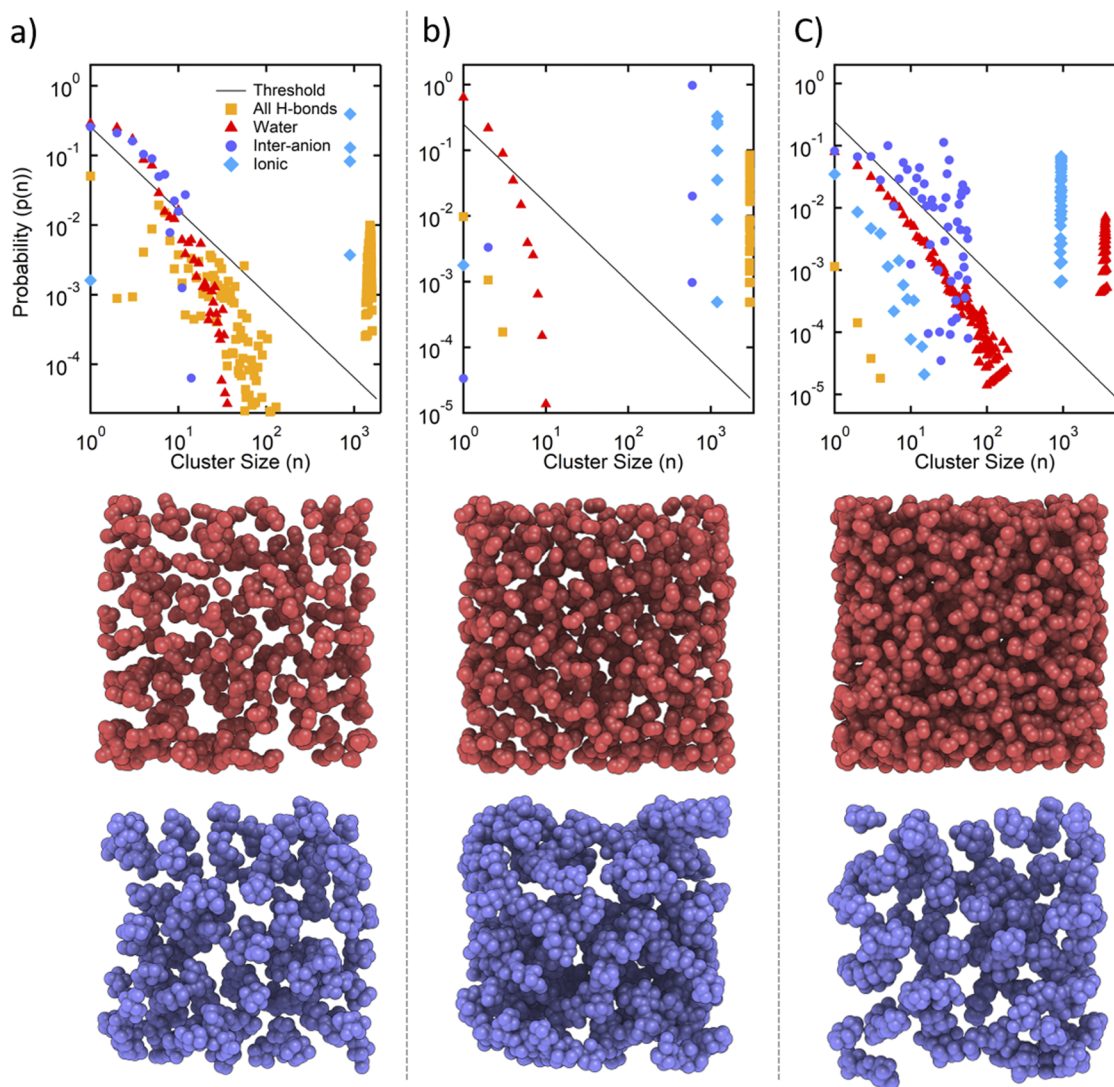


FIG. 5. Cluster analysis of various interactions in (a) choline aspartate + 3 water, (b) choline hydrogen aspartate + 3 water, and (c) choline hydrogen aspartate + 10 water. Probability is the fraction of species in a cluster of size n , defined by separation distances. The solid line shows the theoretical percolation threshold ($p = n^{-1.2}/4.0$, $p = n^{-1.2}/3.9$, and $p = n^{-1.2}/4.1$), where the normalization factor depends on the total number of molecules within each model. The middle row shows representative snapshots of liquid simulation boxes depicting only water molecules (red), and the bottom row shows anions only (violet) as 30 Å thick slices of a 50 × 50 Å² window.

neighbor correlations between water molecules in ChHAsp contrast with the pronounced correlation peak seen at 1.8 Å in Ch₂Asp, where the water is also sufficiently organized for a next-nearest neighbor peak to be visible at 3 Å, just as was seen in ChAc + 5 water. Remarkably, although sufficient water has been added to achieve minimal solvation ChHAsp, but not Ch₂Asp, it is Ch₂Asp that evinces tetrahedral or “bulk” water.

Spatial distribution functions of strong H-bond acceptor oxygens around a water hydrogen show that all H-bonds are short and linear and occupy the same sites (Fig. S4). Therefore, they compete for limited available H-bond donors. Coordination numbers (Table I) show that ~60% of water hydrogens are H-bonded to one of the carboxylate oxygens in both water-lean systems, while ~10% are bonded to the choline hydroxyl. In ChHAsp, only 11% of water hydrogens form water–water H-bonds, whereas in Ch₂Asp, these account for 28%.

These differences are reflected in the propensity of these liquids to form extended H-bonded clusters and networks. Figure 5 shows the probabilities of finding various species within clusters of different sizes within (a) choline aspartate + 3 water, (b) choline hydrogen aspartate + 3 water, and (c) choline hydrogen aspartate + 10 water, compared with the predictions of percolation or random association. In ChHAsp + 3 water [Fig. 5(b)], water is only present in significant amounts as an isolated molecule, a dimer or a trimer, with the probability of larger clusters then falling below the random threshold. This is also seen in the simulation snapshot shown in Fig. 5(b). Neither large clusters nor an extended water network are visible. As seen in reline, the HBD is fully occupied forming strong H-bonds with the cation and anion.⁸ In contrast with water, the HAsp[−] zwitteranion in this system does associate into a continuous, anion–anion H-bonding network that consumes all anions in the simulation box, also seen in the simulation snapshot below Fig. 5(b). The significance of this interaction is underscored by the pair correlation functions for ChHAsp (Fig. 6), which shows a prominent nearest neighbor correlation of the protonated α -ammonium–carboxylate H-bond that is second only to the choline hydroxyl cation–carboxylate anion H-bond.

While a water-only network is absent, an H-bond network that includes all water and salt donor and acceptor interactions also forms a continuous network that includes almost all species present in the simulation box. This suggests that the liquid mixture

is homogenous, with no segregation of water and ion clusters. The primary solvation shell integrates the ions into a network of strong H-bonds involving all species, similar to that seen in reline and other DESs.^{8,10,12}

Figure 5(a) shows the corresponding cluster analysis of Ch₂Asp + 3 water. With the α -amine group deprotonated, the inter-anion network in this system has become discontinuous. Like water, here, the anion only forms small clusters with $n < 10$. Although an overall continuous H-bond network containing both ions and water is still present, deprotonation of the ammonium in Ch₂Asp and the change in H-bond donor–acceptor ratio reduce the anion’s capacity to participate in an H-bond network. Instead, it gives rise to a significant population of large but finite mixed clusters containing several tens of water molecules and ions.

Effect of water content

In their study of the dilution of reline by water, Hammond *et al.* reported a discontinuity in the coordination number between salt to water mole ratios of 1:10 and 1:15, where the choline–choline coordination number reaches a local minimum and salt–water coordination numbers reach a local maximum.²⁵ As a result, the authors concluded that at up to 10:1 (mol:mol) water:salt, the reline–water mixture still possesses some DES characteristics due to the presence of DES clusters. However, further addition of water will lead to a step change in molecular arrangement where most DES motifs dissolve in water. Such a structural transition has also been deduced based on experimental and simulation studies of water dilution of reline,^{8,38,40–44} as well as for 1:2 mol mixtures of choline chloride:ethylene glycol at a lower water content, where a regime of discrete DES clusters dispersed in water was identified between the transition of from DES-like to a concentrate aqueous electrolyte.⁴⁵ Here, we have also investigated the choline hydrogen aspartate + 10 water as a water-rich system in comparison to ChHAsp + 3 water.

Figure 6 compares the atom–atom pair correlation functions of all H-bonding interactions in ChHAsp:water at mole ratios below (1:3) and above (1:10) its eutectic composition. Unsurprisingly, nearest neighbor correlations are more pronounced between water H-bond donors and acceptors with all their counterparts on the cation (hydroxyl), anion (carboxyl), and other water molecules, while correlations between sites on ionic species are diminished to

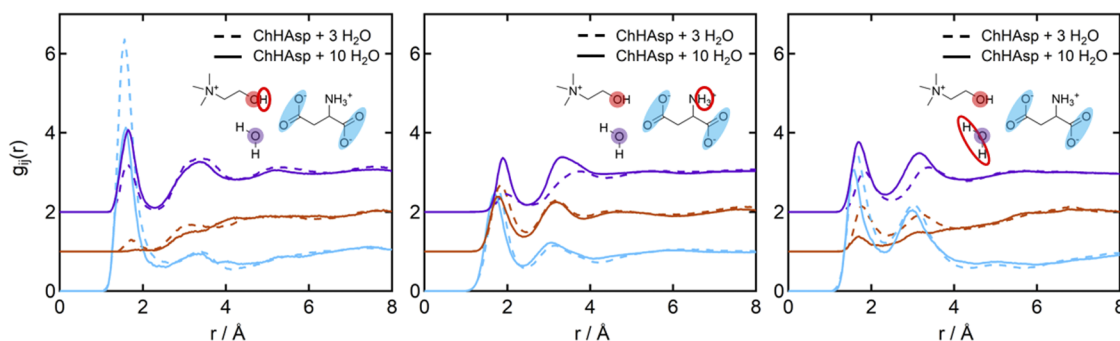


FIG. 6. Atom–atom pair correlation functions between all potential H-bonding pairs within ChHAsp with three waters (dashed) and ten waters (solid). For each panel, the H-bonding hydrogen is circled while different acceptor sites are shaded and color matched to their corresponding pair correlation functions.

some extent. Cation–anion (carboxylate) H-bonding remains the dominant interaction, even at a high water content. Anion–anion H-bonds also retain a significant but reduced presence, while the cation hydroxyl group remains the least important H-bond acceptor. Ammonium–hydroxyl H-bonds are suppressed in the presence of ten waters, while ammonium–carboxylate (anion–anion) correlations are little affected.

Next-nearest neighbor peaks are also visible in several of these pair correlation functions. The second pronounced water–water correlation peak at 3.5 Å again indicates the emergence of tetrahedral water^{35,36} that is not present in ChHAsp with only three waters. A similar tetrahedral arrangement of water may also be inferred around the ammonium donor group. Most other atom–atom pair correlation functions are very similar at the two water contents, suggesting that ChHAsp–water and ion–ion interactions are largely preserved, even up to 10 mol/mol added water. This conclusion is also supported by the coordination numbers listed in Table I. As water is added, there are fewer ion–ion and more water–water H-bonds, although a significant fraction of cation–anion and anion–anion H-bonds remains.

Cluster analysis of ChHAsp + 10 waters [Fig. 5(c)] clearly shows that while the continuous network of all H-bonds seen at a lower water content is retained in this liquid mixture, it differs from the water lean structure in two important ways. First, competition with water suppresses the inter-anion H-bond (ammonium–carboxylate, Table I) so that it can no longer maintain a continuous network of anions alone. It instead forms discrete clusters that contain up to tens of anions. Second, a distinct, continuous, water-only H-bonding network has emerged, replacing the discrete water clusters. This means that ChHAsp + 10 water behaves as a DES–water mixture in which distinct DES clusters exist but are separated by the excess water. This is consistent with the previously reported structure of the dilute aqueous solution of DESs.^{25,45} It also recalls the distinct network formed in water-rich IL–water mixtures,^{35,46} although the present liquid exhibits no long-range amphiphilic nanostructure.

These signatures of bulk water can thus be used to detect the transformation of a DES into a DES-in-water or electrolyte solution (solvated ions) upon dilution. In the former case, all water (or other HBDs) molecules are engaged in H-bonding with the salt, whereas excess water leads first to tetrahedral clusters from which a separate, bulk water network emerges.

CONCLUSIONS

Choline carboxylates and amino acids are promising, biocompatible alternatives to the widely used chloride salt for the preparation of deep eutectic solvents. Water is an effective HBD for DESs, especially when coupled with strong H-bond acceptors, such as carboxylates. The liquid structure, eutectic composition, and how the H-bond network integrates or segregates the choline cation, anion, and water components can all be engineered by changing the ratio of the H-bond donor and acceptor sites. This may be achieved by changing the anion structure or speciation, such as in ChAc vs ChHAsp vs Ch₂Asp, or by changing the mole ratio of salt to water (or other HBDs). This creates the opportunity to design DESs with a specific phase behavior or liquid structure through anion variation as well as fine tuning of their physical properties.

SUPPLEMENTARY MATERIAL

Full atomic labeling, the corresponding Lennard-Jones parameters, and published pK_a values for acetic acid and aspartic acid are listed in the [supplementary material](#) for all our models. Additional radial distribution functions and spatial distribution functions are also provided to support our conclusion.

ACKNOWLEDGMENTS

This work was supported by a Discovery Grant from the Australian Research Council. H.J.J. acknowledges receipt of a Henry Bertie and Florence Mabel Gritton postgraduate scholarship, and S.M. acknowledges receipt of an RTP scholarship from the Australian government. H.J.J. and S.M. acknowledge scholarships from the Australian Institute of Nuclear Science and Engineering. Neutron diffraction measurements were performed at the ISIS Neutron and Muon Source (RAL, UK), SANDALS beamline.

DATA AVAILABILITY

Raw data were generated at the ISIS large scale facility at the Rutherford Appleton Laboratory. Derived data supporting the findings of this study are available from the corresponding author upon reasonable request.

REFERENCES

- 1 A. P. Abbott, G. Capper, D. L. Davies, H. L. Munro, R. K. Rasheed, and V. Tambyrajah, “Preparation of novel, moisture-stable, Lewis-acidic ionic liquids containing quaternary ammonium salts with functional side chains,” *Chem. Commun.* **19**, 2010–2011 (2001).
- 2 L. J. B. M. Kollau, M. Vis, A. van den Bruinhorst, G. de With, and R. Tuinier, “Activity modelling of the solid–liquid equilibrium of deep eutectic solvents,” *Pure Appl. Chem.* **91**(8), 1341–1349 (2019).
- 3 L. J. B. M. Kollau, M. Vis, A. van den Bruinhorst, A. C. C. Esteves, and R. Tuinier, “Quantification of the liquid window of deep eutectic solvents,” *Chem. Commun.* **54**(95), 13351–13354 (2018).
- 4 M. A. R. Martins, S. P. Pinho, and J. A. P. Coutinho, “Insights into the nature of eutectic and deep eutectic mixtures,” *J. Solution Chem.* **48**(7), 962–982 (2019).
- 5 O. Shayestehpour and S. Zahn, “Molecular features of reline and homologous deep eutectic solvents contributing to nonideal mixing behavior,” *J. Phys. Chem. B* **124**(35), 7586–7597 (2020).
- 6 L. Fernandez, L. P. Silva, M. A. R. Martins, O. Ferreira, J. Ortega, S. P. Pinho, and J. A. P. Coutinho, “Indirect assessment of the fusion properties of choline chloride from solid–liquid equilibria data,” *Fluid Phase Equilib.* **448**, 9–14 (2017).
- 7 X. Meng, K. Ballerat-Busserolles, P. Husson, and J.-M. Andanson, “Impact of water on the melting temperature of urea plus choline chloride deep eutectic solvent,” *New J. Chem.* **40**(5), 4492–4499 (2016).
- 8 O. S. Hammond, D. T. Bowron, and K. J. Edler, “Liquid structure of the choline chloride–urea deep eutectic solvent (reline) from neutron diffraction and atomistic modelling,” *Green Chem.* **18**(9), 2736–2744 (2016).
- 9 A. Paiva, R. Craveiro, I. Aroso, M. Martins, R. L. Reis, and A. R. C. Duarte, “Natural deep eutectic solvents—Solvents for the 21st century,” *ACS Sustainable Chem. Eng.* **2**(5), 1063–1071 (2014).
- 10 A. Faraone, D. V. Wagle, G. A. Baker, E. C. Novak, M. Ohl, D. Reuter, P. Lunkenheimer, A. Loidl, and E. Mamontov, “Glycerol hydrogen-bonding network dominates structure and collective dynamics in a deep eutectic solvent,” *J. Phys. Chem. B* **122**(3), 1261–1267 (2018).
- 11 B. B. Hansen, S. Spittle, B. Chen, D. Poe, Y. Zhang, J. M. Klein, A. Horton, L. Adhikari, T. Zelovich, B. W. Doherty, B. Gurkan, E. J. Maginn, A. Ragauskas, M. Dadmun, T. A. Zawodzinski, G. A. Baker, M. E. Tuckerman, R. F. Savinell, and J. R. Sangoro, “Deep eutectic solvents: A review of fundamentals and applications,” *Chem. Rev.* **121**(3), 1232–1285 (2021).

- ¹²O. S. Hammond, D. T. Bowron, A. J. Jackson, T. Arnold, A. Sanchez-Fernandez, N. Tsapatsaris, V. G. Sakai, and K. J. Edler, "Resilience of malic acid natural deep eutectic solvent nanostructure to solidification and hydration," *J. Phys. Chem. B* **121**(31), 7473–7483 (2017).
- ¹³M. E. Di Pietro, O. Hammond, A. van den Bruinhorst, A. Mannu, A. Padua, A. Mele, and M. C. Gomes, "Connecting chloride solvation with hydration in deep eutectic systems," *Phys. Chem. Chem. Phys.* **23**(1), 107–111 (2021).
- ¹⁴X.-D. Hou, Q.-P. Liu, T. J. Smith, N. Li, and M.-H. Zong, "Evaluation of toxicity and biodegradability of cholinium amino acids ionic liquids," *PLoS One* **8**(3), e59145–e59148 (2013).
- ¹⁵Q.-P. Liu, X.-D. Hou, N. Li, and M.-H. Zong, "Ionic liquids from renewable biomaterials: Synthesis, characterization and application in the pretreatment of biomass," *Green Chem.* **14**(2), 304–307 (2012).
- ¹⁶M. Petkovic, J. L. Ferguson, H. Q. N. Gunaratne, R. Ferreira, M. C. Leitão, K. R. Seddon, L. P. N. Rebelo, and C. S. Pereira, "Novel biocompatible cholinium-based ionic liquids-toxicity and biodegradability," *Green Chem.* **12**(4), 643–649 (2010).
- ¹⁷S. Miao, J. Wood, H. J. Jiang, S. Imberti, R. Atkin, and G. Warr, "Unusual origin of choline phenylalaninate ionic liquid nanostructure," *J. Mol. Liq.* **319**, 114327 (2020).
- ¹⁸A. Le Donne, H. Adenusi, F. Porcelli, and E. Bodo, "Structural features of cholinium based protic ionic liquids through molecular dynamics," *J. Phys. Chem. B* **123**(26), 5568–5576 (2019).
- ¹⁹S. De Santis, G. Masci, F. Casciotta, R. Caminiti, E. Scarpellini, M. Campetella, and L. Gontrani, "Cholinium-amino acid based ionic liquids: A new method of synthesis and physico-chemical characterization," *Phys. Chem. Chem. Phys.* **17**, 20687–20698 (2015).
- ²⁰S. Miao, R. Atkin, and G. G. Warr, "Amphiphilic nanostructure in choline carboxylate and amino acid ionic liquids and solutions," *Phys. Chem. Chem. Phys.* **22**(6), 3490–3498 (2020).
- ²¹T. Q. To, K. Shah, P. Tremain, B. A. Simmons, B. Moghtaderi, and R. Atkin, "Treatment of lignite and thermal coal with low cost amino acid based ionic liquid-water mixtures," *Fuel* **202**, 296–306 (2017).
- ²²H. J. Jiang, S. Miao, S. Imberti, B. A. Simmons, R. Atkin, and G. G. Warr, "Liquid nanostructure of choline lysinate with water and a model lignin residue," *Green Chem.* **23**(2), 856–866 (2021).
- ²³X.-D. Hou, N. Li, and M.-H. Zong, "Facile and simple pretreatment of sugar cane bagasse without size reduction using renewable ionic liquids-water mixtures," *ACS Sustainable Chem. Eng.* **1**(5), 519–526 (2013).
- ²⁴C. F. Carrozza, G. Papa, A. Citterio, R. Sebastiano, B. A. Simmons, and S. Singh, "One-pot bio-derived ionic liquid conversion followed by hydrogenolysis reaction for biomass valorization: A promising approach affecting the morphology and quality of lignin of switchgrass and poplar," *Bioresour. Technol.* **294**, 122214 (2019).
- ²⁵O. S. Hammond, D. T. Bowron, and K. J. Edler, "The effect of water upon deep eutectic solvent nanostructure: An unusual transition from ionic mixture to aqueous solution," *Angew. Chem., Int. Ed.* **56**(33), 9782–9785 (2017).
- ²⁶C. D'Agostino, L. F. Gladden, M. D. Mantle, A. P. Abbott, E. I. Ahmed, A. Y. M. Al-Murshedi, and R. C. Harris, "Molecular and ionic diffusion in aqueous—Deep eutectic solvent mixtures: Probing inter-molecular interactions using PFG NMR," *Phys. Chem. Chem. Phys.* **17**(23), 15297–15304 (2015).
- ²⁷X.-D. Hou, T. J. Smith, N. Li, and M.-H. Zong, "Novel renewable ionic liquids as highly effective solvents for pretreatment of rice straw biomass by selective removal of lignin," *Biotechnol. Bioeng.* **109**(10), 2484–2493 (2012).
- ²⁸D. Lapena, F. Bergua, L. Lomba, B. Giner, and C. Lafuente, "A comprehensive study of the thermophysical properties of reline and hydrated reline," *J. Mol. Liq.* **303**, 112679 (2020).
- ²⁹Y. Wang, C. Ma, C. Liu, X. Lu, X. Feng, and X. Ji, "Thermodynamic study of choline chloride-based deep eutectic solvents with water and methanol," *J. Chem. Eng. Data* **65**(5), 2446–2457 (2020).
- ³⁰A. K. Soper, W. S. Howells, and A. C. Hannon, ATLAS—Analysis of Time-of-Flight Diffraction Data from Liquid and Amorphous Samples RAL-89-046, 1989.
- ³¹A. K. Soper, "Empirical potential Monte Carlo simulation of fluid structure," *Chem. Phys.* **202**, 295 (1996).
- ³²E. P. Serjeant and B. Dempsey, *Ionisation Constants of Organic Acids in Aqueous Solution* (Pergamon Press, Oxford; New York, 1979).
- ³³S. McDonald, T. Murphy, S. Imberti, G. G. Warr, and R. Atkin, "Amphiphilically nanostructured deep eutectic solvents," *J. Phys. Chem. Lett.* **9**(14), 3922–3927 (2018).
- ³⁴A. Le Donne, H. Adenusi, F. Porcelli, and E. Bodo, "Hydrogen bonding as a clustering agent in protic ionic liquids: Like-charge vs opposite-charge dimer formation," *ACS Omega* **3**(9), 10589–10600 (2018).
- ³⁵M. Brunner, S. Imberti, B. A. Simmons, G. G. Warr, and R. Atkin, "Liquid nanostructure of cholinium arginate biomass solvents," *ACS Sustainable Chem. Eng.* **9**(7), 2880–2890 (2021).
- ³⁶A. K. Soper, "The radial distribution functions of water as derived from radiation total scattering experiments: Is there anything we can say for sure?," *Int. Scholarly Res. Not.* **2013**, 279463.
- ³⁷A. K. Soper, "The radial distribution functions of water and ice from 220 to 673 K and at pressures up to 400 MPa," *Chem. Phys.* **258**(2-3), 121–137 (2000).
- ³⁸L. Sapir and D. Harries, "Restructuring a deep eutectic solvent by water: The nanostructure of hydrated choline chloride/urea," *J. Chem. Theory Comput.* **16**(5), 3335–3342 (2020).
- ³⁹M. V. Fedotova, S. E. Kruchinin, and G. N. Chuev, "Features of local ordering of biocompatible ionic liquids: The case of choline-based amino acid ionic liquids," *J. Mol. Liq.* **296**, 112081 (2019).
- ⁴⁰Y. Xie, H. Dong, S. Zhang, X. Lu, and X. Ji, "Effect of water on the density, viscosity, and CO₂ solubility in choline chloride/urea," *J. Chem. Eng. Data* **59**(11), 3344–3352 (2014).
- ⁴¹D. Shah and F. S. Mjalli, "Effect of water on the thermo-physical properties of Reline: An experimental and molecular simulation based approach," *Phys. Chem. Chem. Phys.* **16**(43), 23900–23907 (2014).
- ⁴²P. Kumari, Shobhna, S. Kaur, and H. K. Kashyap, "Influence of hydration on the structure of reline deep eutectic solvent: A molecular dynamics study," *ACS Omega* **3**(11), 15246–15255 (2018).
- ⁴³Q. Gao, Y. Zhu, X. Ji, W. Zhu, L. Lu, and X. Lu, "Effect of water concentration on the microstructures of choline chloride/urea (1:2)/water mixture," *Fluid Phase Equilib.* **470**, 134–139 (2018).
- ⁴⁴E. O. Fetisov, D. B. Harwood, I.-F. W. Kuo, S. E. E. Warrag, M. C. Kroon, C. J. Peters, and J. I. Siepmann, "First-principles molecular dynamics study of a deep eutectic solvent: Choline chloride/urea and its mixture with water," *J. Phys. Chem. B* **122**(3), 1245–1254 (2018).
- ⁴⁵S. Kaur, A. Gupta, and H. K. Kashyap, "How hydration affects the microscopic structural morphology in a deep eutectic solvent," *J. Phys. Chem. B* **124**(11), 2230–2237 (2020).
- ⁴⁶R. Hayes, S. Imberti, G. G. Warr, and R. Atkin, "How water dissolves in protic ionic liquids," *Angew. Chem., Int. Ed.* **51**(30), 7468–7471 (2012).